Self-organized coexistence of phage and a population of host colonies

Anjali Yadav, Namiko Mitarai, and Kim Sneppen
Niels Bohr Institute, University of Copenhagen, Denmark

(Dated: September 2, 2024)

Phages and bacteria coexist under widely different conditions, ranging from liquid cultures to oceans, soil, and the human gut. However, our models are typically limited to well-mixed liquid cultures governed by mass-action kinetics. Here, we suggest a modification to the Lotka-Volterra dynamics by including the formation of microcolonies. By analyzing the model in an open system with a steady influx of bacteria, we predict that the colony size distribution is power-low distributed with steeper exponents for the stronger external influx. In the realistic case where the phage attack rate to individual colonies is proportional to their radius, we obtain self-organization to a steady state where the maximal colony size is smaller for stronger external driving.

The co-existence of bacteria and its virulent phage was predicted already by Cambell [1] and later confirmed experimentally in continuous chemostat culture [2, 3] as well as by serial transfer [4]. However, the predator-prey relationship between phage and host is destabilized by the many off-spring phages from each infected bacterium, suggesting that well-mixed conditions should have extreme oscillations that may easily lead to the extinction of the host population [5]. These extreme oscillations are often not observed in experimental data [2], perhaps because the bacterial liquid culture tends to develop heterogeneity associated with some bacteria growing on the glass walls of the chemostat [4]. Here we will introduce a model for another spatial heterogeneity, using the fact that many bacteria types tend to grow in clusters and that these clusters provide some spatial refuge against phages [5–7].

As a wide-ranging goal, we aim to develop a better understanding of diversity and coexistence within ecological systems. Commonly, researchers employ mean-field models to interpret the associated dynamics, using generalizations and extensions of the famous Lotka-Volterra (LV) framework [8, 9]. While these equations have given us much insight into concepts like the competitive exclusion principle [10–14], they tend to be too fragile to support the co-existence of many competing species. To remedy these deficiencies, Robert Holt [15] suggested that spatial heterogeneity is important for stabilizing ecosystems. From this perspective, the current paper explores conditions where clusters of prey may self-organize to help their population evade predators more effectively, thereby stabilizing their overall numbers.

We initiate our study by considering the standard LV form of predator-prey modelling, which mathematically studies the temporal evolution of bacterial $B(t)$ and phage $P(t)$ populations in a well-mixed system. The key assumptions of LV equations are that the populations are evenly spread out over the entire habitat and interactions between predators and prey occur randomly and uniformly. Each predator is equally likely to encounter any prey individual at any time. We extend the conventional LV framework by suggesting a model where each bacterium can develop into a distinct microcolony as bacteria grow, thereby introducing a microcolony-based modification to the interaction dynamics. This model alteration suggests a shift from a model of distributed individual bacteria and phages to one featuring distributed microcolonies and phages, enhancing the complexity and realism of the model.

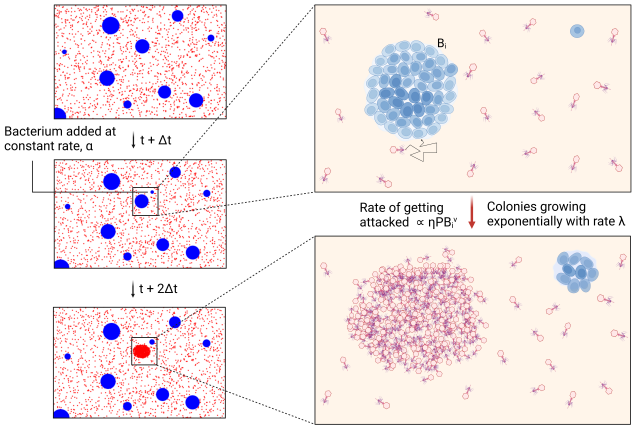

FIG. 1. Schematic description of the model. A new bacterium is introduced to the system at a rate α per volume, and each bacterium grows exponentially at a rate λ to form a colony (blue circles). A colony of population B_i is attacked by a phage (red dots, density P) at a rate $\eta P B_i^{\nu}$. The phage attack results in all the bacteria in the colony eventually being infected, producing βB_i new free phages. Free phage decays at a rate δ.

Model. A schematic representation of the model is illustrated in Fig. 1, where each sphere symbolizes a microcolony of bacteria. We use a well-mixed model of microcolonies and phages in the system, disregarding other spatial considerations. The system has an influx of individual bacteria with a rate α. Each bacteria being added to the system may subsequently grow into a microcolony. Bacteria in microcolonies have a constant growth rate of λ, implicitly assuming a constant resource per bacteria. The rate at which a phage infects a colony depends on the

size of the colony (B), infection rate (η) and phage density (P). We assume the rate is given by $\eta P B^{\nu}$, where we later motivate the value for the exponent ν. Each infection event results in an instantaneous colony burst with the release of β (burst size) phages per bacterium of the colony. This is a simplification where we ignore the latency time for the phage production and assume that the phages produced by infected bacteria immediately reinfect other bacteria in the system to burst all the cells eventually. Finally, the free phage decays slowly at a constant rate δ. Thus, the system is slowly driven by bacteria addition and dissipated by sudden colony infection and collapse.

We simulate the dynamics of phage-bacteria interactions in a system where each bacterial colony i ($i = 1, \ldots, N$) is modelled as a discrete entity. The overall phage density P and the population size of bacteria within each colony B_i are treated as continuous variables, and phage decay and bacteria growth are simulated deterministically. The simulation proceeds with a discrete time step Δt. During each time step, the following stochastic event can happen in addition to the deterministic growth and decay dynamics: 1) A single bacterium is added to the system at a rate α per unit volume, starting a new colony. 2) Each colony i is subject to infection events with a rate $\eta P B_i^{\nu}$. When the infection happens, the colony is removed, and βB_i phages are produced.

The corresponding mean field equations are:

$$\dot{B}_i = \lambda B_i \;\; for \;\; i = 1, 2, ...N, \tag{1}$$

$$\dot{P} = \frac{\beta\eta}{V} \sum_{i=1}^{N} B_i^{\nu} P - \delta P, \tag{2}$$

with the colony number density ρ described by

$$\dot{\rho} = \alpha - \eta P \rho. \tag{3}$$

Here, V is the system's volume, and N is the total number of colonies in the system.

We study the system for two cases. $\nu = 0$ represents the infection rate of colonies independent of colony size. However, in a well-mixed liquid culture, a colony's attack rate is expected to be determined by diffusion-limited search. If so, the adsorption rate is proportional to the radius of the target, which for a colony of size B would scale as $B^{1/3}$ [16]. Therefore, we consider the $\nu = 1/3$ case, as it was confirmed experimentally by Ref. [17].

Unless otherwise noted, we use $\eta = 10^{-8} ml/h$, $\lambda = 2h^{-1}, \delta = 0.1h^{-1}, \beta = 100$. These values are realistic ranges for typical *E. coli* phages [18, 19]. The time step is set to $\Delta t = 10^{-4}$ h, which is small enough to ensure that the probability for stochastic events happening per Δt does not exceed 1. To simulate the system stochastically, we also have the total system size V as an additional parameter, which we set to $V = 1L$ unless otherwise noted. The value of α is varied to explore the effect of the influx.

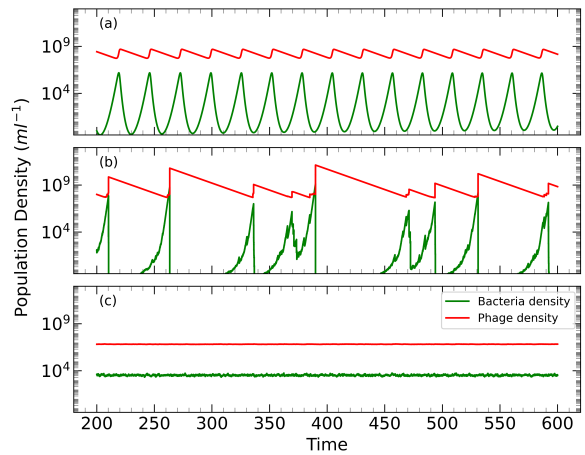

FIG. 2. Temporal dynamics of bacterial and phage population density simulated using the Gillespie algorithm for three different models: (a) the Lotka-Volterra (LV) model, (b) the model with $\nu = 0$, and (c) the model with $\nu = 1/3$, illustrating more stable population densities. Phage parameters are $\eta = 10^{-8}, \lambda = 2h^{-1}, \delta = 0.1h^{-1}, \beta = 100$. Simulations use $V = 1L$ and $\alpha = 0.1h^{-1}ml^{-1}$. The near-constant dynamics in panel C) are replaced by episodic bust-boom dynamics when $\alpha \cdot V \sim 1/h$ (See Fig. S5).

Population dynamics. Model dynamics is shown in Fig 2. For comparison, panel (a) illustrates the characteristic oscillatory dynamics of the simplified LV version of the model where bacteria do not form colonies. Panel (b) shows the dynamics when considering $\nu = 0$, where episodic population dynamics is associated with the collapse of individual large colonies. Panel (c) presents the more realistic case with $\nu = 1/3$. Here, the populations of both phage and bacteria become stabilized.

Panel b) shows a repeated pattern of bacterial population growth followed by sudden drops associated with phage attacks. Complementary to these, one observes sudden increases in phage density followed by exponential decay set by δ. When the phages eventually infect a sufficiently large colony, there is a sudden spike in phage density, which hugely increases the attack rate on all other colonies, leading to their nearly simultaneous collapse. Subsequently, the many phages prevent even the smallest colonies from surviving. Once the phage density decreases to a sufficiently low level, the colonies can begin to grow again, and the cycle repeats.

When we assume $\nu = 1/3$ the dynamics stabilize, as seen in panel c). The colonies grow but are eliminated before they become substantial. This is because larger colonies are more easily found and eliminated by the phages. As a result, the phages keep the system in check and prevent any single colony from dominating due to its size. This then prevents the extreme spike of the phage density, reducing the fluctuation. In fact, the fluctuations will increase if α or phage adsorption rate η are

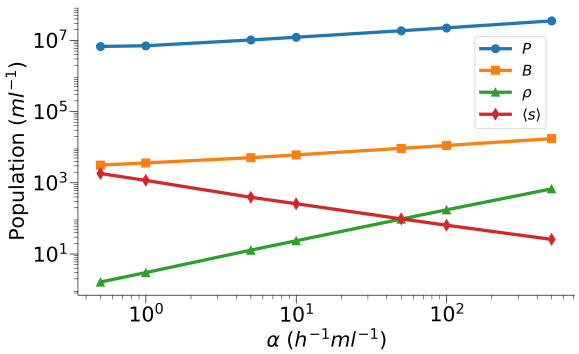

FIG. 3. Dependence of phage population density(P), bacterial population density(B), colony density ρ, and average colony size $\langle s\rangle$ on the bacteria introduction rate α for a system of $V = 10$ ml for $\nu = 1/3$. The graph illustrates the inverse relationship between α and both bacterial population and density while showing an increase in average colony size with higher α, highlighting the complex dynamics of bacterial-phage interactions.

very small, as explored in supplementary figure ($S6, S7$).

A central parameter in our model is the rate of addition of individual bacteria α. In Figure 3, we show the α dependence of the densities of phages (P) and bacteria (B) per unit volume, the number density of colonies ρ per unit volume for $\nu = 1/3$ case. $\langle s\rangle$ shows the average size of colonies. Interestingly, the relative change in P is much less than the relative change in $\langle s\rangle$ and ρ. As we increase the driving rate α, $\langle s\rangle$ decreases, and ρ increases, balancing the overall population density. This shows that it is a driving and dissipative system that self-organises itself so that the steady-state population remains approximately the same.

Colony size distribution. To analytically study the system, let us consider $n(s)$ as the density of colonies of size s in the system at time t. The temporal evolution of $n(s)$ is given by the following master equation:

$$\dot{n}(s) = \lambda(s-1)n(s-1) - \lambda s n(s) - \eta P s^{\nu} n(s), \quad (4)$$
$$\dot{n}(1) = \alpha - \lambda n(1) - \eta P n(1). \quad (5)$$

The dynamics of phage density (P) is given by:

$$\dot{P} = \beta \sum_{s=1}^{\infty} \eta P s^{\nu} n(s) - \delta P. \quad (6)$$

For the first model, $\nu = 0$, we do not have a constant steady-state phage density. However, we observed that the instantaneous probability distribution of the colony size at time t obeys (Supplementary Fig. S1)

$$n(s|s_{max}) = s^{-\gamma(s_{max})} H(s_{\max} - s) \quad (7)$$

where $H(x)$ is the Heaviside step function. The distribution of the exponent $\gamma(s_{max})$ for different values of α is explored in Supplementary Fig. S3. The time-averaged $n(s)$ will then be given by

$$n(s) = \int_1^{\infty} n(s|s_{max})\mathcal{P}(s_{max}) ds_{max}. \quad (8)$$

where $\mathcal{P}(s_{max})$ is probability distribution of s_{max}. We evaluated $\mathcal{P}(s_{max})$ from the simulation data (Supplementary Fig. S3) as $\mathcal{P}(s_{max}) \propto s_{max}^{-r}$ and integrated eq. (8) (supplementary text sec. S1). This gave us a power-law distribution

$$n(s) \propto s^{-\tau} \quad (9)$$

with a logarithmic correction. The simulation data indeed show power-law distributions over 4 decades with exponent τ between 1.3 and 1.5 depending on α (Fig. 4a).

For $\nu = 1/3$, the system reaches a steady-state. Ignoring the fluctuations in P and solving equation eq. (4) for a steady-state, and approximating $(s-1)n(s-1) - sn(s) \approx -\frac{d(sn(s))}{ds}$, we obtain

$$\frac{d(sn(s))}{ds} = -\frac{\eta P s^{1/3}}{\lambda} n(s).$$

Solving this gives us

$$n(s) = \mathcal{N} \exp\left(-3\frac{\eta}{\lambda} P \cdot s^{1/3}\right) \cdot \frac{1}{s} \quad (10)$$

with a normalisation constant $\mathcal{N}$. The equation indicates a power-law decay, $n(s) \propto s^{-1}$ moderated by the size-dependent cutoff reflecting increased vulnerability to phage attacks as colony size increases.

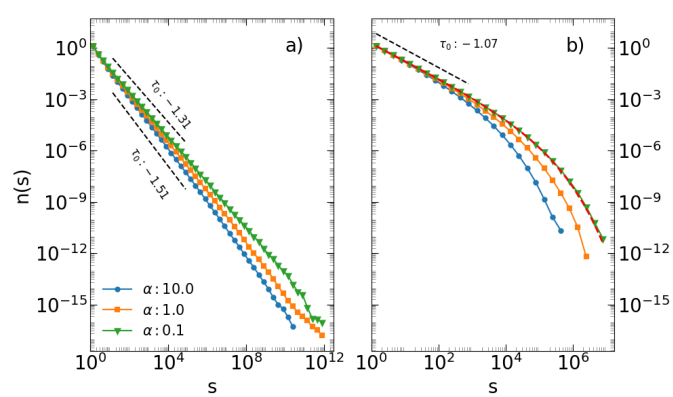

FIG. 4. Normalised time averaged colony size distribution in steady state for different values of bacteria introduction rate α. a) Model with $\nu = 0$. b) Model with $\nu = 1/3$. The analytical solution (10) is shown as a red dashed line in the plot b).

The analytical result eq. (10) shows an excellent agreement with numerical simulations as shown in Fig. 4b. The agreement is particularly strong for smaller values of α, specifically as $\alpha \to 0$.

Discussion. Inspired by phage-bacteria systems, this paper explored Lotka-Volterra dynamics with a prey population partitioned into colonies. When each single bacteria grows to form a micro-colony, the resulting population is much more difficult for the phage to find [20, 21]. If the chance of finding a colony stays constant per phage, the model predicts the power-law distribution of colony size with exponent τ around 1.5. With a more realistic Smouluchowski relation of 3-dimensional diffusion limited search, the chance to localize the colony grows with the cube root of its population [17, 22], making a larger colony easier to find. This results in the cut-off of otherwise power-law distributed colony size of exponent 1 (Fig. 4), reducing the fluctuation of the steady state population (Fig. 2). Interestingly, the system self-organises the colony number and colony size so that the phage and bacteria population change little against the changes in bacteria influx (Fig. 3), predicting relatively a constant value of the phage-to-bacterial ratio.

In many natural habitats, the phage-to-bacterial ratio (P/B) becomes substantially below the factor 10 [23], while our current simulations (e.g. Fig. 3) give a fairly large value of $P/B \approx 2 \times 10^3$. This value is identical to the steady-state mean field value, $P/B = \lambda\beta/\delta = 2 \times 100/0.1 = 2000$. To obtain smaller ratios, β should be smaller or λ/δ relatively small.

There are a few additional features of the model assumption which could be alleviated to reduce this discrepancy in the P/B ratio.

We have neglected the travel time associated with spatial heterogeneity in the system. When the colony concentration is low, the phages produced upon the burst of a colony need to locate a new colony. This gives more time for colonies to grow, and phages can decay while travelling. We simulated this situation by considering spatiotemporal dynamics in two dimensions, where bacteria colonies do not move but phages diffuse [24] (Supplementary Text S6, Fig S12). For a small α where the colony density is low, and the carrying capacity dominates the maximum colony size, we observed a drop of P/B.

Our model also neglected the dynamics of the process where phages penetrate a colony by repeated infection and replication and simplified it as one phage attack immediately results in the entire colony burst. We studied the effect of time delay in this process by simulating a version of the model where the burst of a bacterium in an attacked colony happens at a constant burst rate per bacterium, resulting in an exponential decay of colony size over time (Supplementary text $S5$). This reduces the severity of the phage attack, and when we conservatively assume this decay rate to be $\ln 10/\mathrm{h}$, we predict a factor 2 decrease in the P/B ratio (Supplementary Fig $S11$ and $S12$).

There are further physical constraints when phages attack a colony from outside. The spread of infection is limited by superinfected surface cells [7, 25, 26] and/or hindered by an extracellular matrix which can trap phages [27]. Such limits on the phage predation naturally reduce P and increase B, again bringing the P/B ratio down.

The feature of hiding the prey population in clusters in plain sight may have analogues in other parts of the living world. Fish aggregate in schools to minimize predator attacks [28], while cicadas satiate their predators during their rare but synchronous swarming events [29]. Our simplest scenario considers an extreme version of heterogeneity, where the predator's ability to localize a colony was independent of its size. This perspective of replacing an attack rate dependent of $size^{1/3}$ with a constant is analogue to the difference between the "dynamic kill the winner" model of [30] and the simple Boom-Bust model of [31]. Taking into account the phage versus colony dynamics, our model enhances the magnitude and duration of the "busts" because the collapse of a large colony is followed by a prolonged period of phage dominance where no bacteria persist.

In summary, we introduced a minimal stochastic model for phages spreading in a population of hosts that is partitioned into colonies. In particular, we highlight a self-organization of colony size and number at different exposures to the surrounding environment. The model inspires further studies of phage travel time between colonies, which in the case of *Vibrio* species in the ocean should include hydrodynamic mixing above the Kolmogorov scale of about a few mm. When considering the observation of a large diversity of coexisting phages and their host in the ocean [32], our model suggests that this is a result of individual bacteria species that boom in the form of colony growth on a preferred nutrient followed by a bust due to rare infection by a scarce phage. This is consistent with data of *Vibrio* species and their phages [32] where snapshots of populations of individual phage species most often are below 0.1 phages per ml but sometimes count up to 40 phages per ml. It is also worth mentioning that colony or aggregate formation and dispersal are often quorum sensing regulated [33, 34], allowing the bacteria to regulate the colony size depending on the environmental clues. It is an interesting future question to understand how colony formation and dispersion regulate the phage-bacteria populations.

Acknowledgment: This research was funded by the Novo Nordisk Foundation (NNF21OC0068775) and the Danish National Research Foundation (grant no. DNRF170).

[1] A. Campbell, Conditions for the Existence of Bacteriophage, Evolution **15**, 153–165 (1961).

[2] B. Levin, F. Stewart, and L. Chao, Resource-Limited Growth, Competition, and Predation: A Model and Experimental Studies with Bacteria and Bacteriophage, The American Naturalist **111**, 3–24 (1977).

[3] B. J. Bohannan and R. E. Lenski, Effect of resource enrichment on a chemostat community of bacteria and bacteriophage, Ecology **78**, 2303 (1997).

[4] S. Schrag and J. Mittler, Host-parasite coexistence: the role of spatial refuges in stabilizing bacteria-phage interactions, The American Naturalist **148**, 348 (1996).

[5] S. Heilmann, K. Sneppen, and S. Krishna, Coexistence of phage and bacteria on the boundary of self-organized refuges, Proceedings of the National Academy of Sciences of the United States of America **109**, 12828–12833 (2012).

[6] R. S. Eriksen, N. Mitarai, and K. Sneppen, Sustainability of spatially distributed bacteria-phage systems, Scientific reports **10**, 3154 (2020).

[7] R. S. Eriksen, F. Larsen, S. L. Svenningsen, K. Sneppen, and N. Mitarai, The dynamics of phage predation on a microcolony, Biophysical Journal **123**, 147 (2024).

[8] A. Lotka, *Elements of Physical Biology* (Williams and Wilkins., 1925).

[9] V. Volterra, Variazioni e fluttuazioni del numero d'individui in specie animali conviventi, Memoria della regia accademia nazionale del lincei ser. **2**, 31–113 (1926).

[10] G. Gause, The Struggle for Existence, Soil Science **41**, 159 (1936).

[11] G. Hardin, The competitive exclusion principle, Science **131**, 1292–1297 (1960).

[12] S. Levin, Community Equilibria and Stability, and an Extension of the Competitive Exclusion Principle, The American Naturalist **104**, 413–423 (1970).

[13] J. O. Haerter, N. Mitarai, and K. Sneppen, Phage and bacteria support mutual diversity in a narrowing staircase of coexistence, The ISME journal **8**, 2317 (2014).

[14] J. O. Haerter, N. Mitarai, and K. Sneppen, Food web assembly rules for generalized lotka-volterra equations, PLoS computational biology **12**, e1004727 (2016).

[15] R. Holt, Spatial heterogeneity, indirect interactions, and the coexistence of prey species., American Naturalist (1984).

[16] H. Berg and E. Purcell, Physics of chemoreception, Biophysical Journal **20**, 193 (1977).

[17] K. Sneppen, I. Østerlund, S. Svenningsen, and S. Brown, Synthetic biology for vector-borne diseases, PRX Life **1**, 013015 (2023).

[18] M. De Paepe and F. Taddei, Viruses' life history: towards a mechanistic basis of a trade-off between survival and reproduction among phages, PLoS biology **4**, e193 (2006).

[19] R. T. Noble and J. A. Fuhrman, Virus decay and its causes in coastal waters, Applied and Environmental Microbiology **63**, 77 (1997).

[20] S. T. Abedon, Spatial vulnerability: bacterial arrangements, microcolonies, and biofilms as responses to low rather than high phage densities, Viruses **4**, 663 (2012).

[21] R. S. Eriksen, N. Mitarai, and K. Sneppen, On phage adsorption to bacterial chains, Biophysical Journal **119**, 1896 (2020).

[22] M. Von Smoluchowski, Zur kinetischen theorie der brownschen molekularbewegung und der suspensionen, Annalen der physik **326**, 756 (1906).

[23] M. G. Weinbauer, Ecology of prokaryotic viruses, FEMS microbiology reviews **28**, 127 (2004).

[24] R. Moldovan, E. Chapman-McQuiston, and X. L. Wu, On kinetics of phage adsorption, Biophysical Journal **93**, 303 (2007).

[25] B. P. Taylor, C. J. Penington, and J. S. Weitz, Emergence of increased frequency and severity of multiple infections by viruses due to spatial clustering of hosts, Physical biology **13**, 066014 (2017).

[26] R. S. Eriksen, S. L. Svenningsen, K. Sneppen, and N. Mitarai, A growing microcolony can survive and support persistent propagation of virulent phages, Proceedings of the National Academy of Sciences **115**, 337 (2018).

[27] L. Vidakovic, P. K. Singh, R. Hartmann, C. D. Nadell, and K. Drescher, Dynamic biofilm architecture confers individual and collective mechanisms of viral protection, Nature microbiology **3**, 26 (2018).

[28] B. L. Partridge, The structure and function of fish schools, Scientific american **246**, 114 (1982).

[29] K. S. Williams, K. G. Smith, and F. M. Stephen, Emergence of 13-yr periodical cicadas (cicadidae: Magicicada): Phenology, mortality, and predators satiation, Ecology **74**, 1143 (1993).

[30] S. Maslov and K. Sneppen, Population cycles and species diversity in dynamic kill-the-winner model of microbial ecosystems, Scientific reports **7**, 1 (2017).

[31] S. Maslov and K. Sneppen, Diversity waves in collapse-driven population dynamics, PLoS computational biology **11**, e1004440 (2015).

[32] K. M. Kauffman, W. K. Chang, J. M. Brown, F. A. Hussain, J. Yang, M. F. Polz, and L. Kelly, Resolving the structure of phage–bacteria interactions in the context of natural diversity, Nature communications **13**, 372 (2022).

[33] P. K. Singh, S. Bartalomej, R. Hartmann, H. Jeckel, L. Vidakovic, C. D. Nadell, and K. Drescher, Vibrio cholerae combines individual and collective sensing to trigger biofilm dispersal, Current Biology **27**, 3359 (2017).

[34] E. L. Bruger and C. M. Waters, Maximizing growth yield and dispersal via quorum sensing promotes cooperation in vibrio bacteria, Applied and environmental microbiology **84**, e00402 (2018).